Bacterial Diterpene Synthases: A Tale of Two Conserved Domains

This report features the work of Rey-Ting Guo, Eric Oldfield and their co-workers published in J. Am. Chem. Soc. ***136****, 2892 (2014) and Sci. Rep.* ***4****, 6214 (2014).*

Terpenes (or terpenoids) represent the largest class of small molecules on the planet. About 20% of terpenes are diterpenes, molecules that contain a core of 20 carbon atoms, and most are made by plant and fungal enzymes. Diterpenes are, however, also found in bacteria, and several of these compounds have activity as anti-infective and anti-cancer drug leads and virulence factors, as well as plant growth hormones.

The structures and mechanism of action of terpene synthases have been studied for many years, but the first structures of diterpene synthases were unreported until 2011.[1,2] These are two diterpene cyclases from plants and adopt an "αβγ" three-helical conserved domain structure.[1,2] It was proposed that the plant αβγ domain proteins arose by fusion of the genes of ancestral α and βγ domain synthases in soil-dwelling bacteria, but no structures of bacterial diterpene synthases have been reported.

To understand bacterial diterpene synthases better, Rey-Ting Guo, Eric Oldfield and their co-workers solved two bacterial diterpene synthase structures: virulence-associated enzyme (Rv3378c) from *Mycobacterium tuberculosis*[3] and *ent*-kaurene synthase (BjKS) from soil bacterium *Bradyrhizobium japonicum*.[4] The former protein is of interest as its product (1-tuberculosinyl adenosine) is a virulence factor for *M. tuberculosis*, and, hence, targets for anti-virulence-based therapies.[5] The latter is of interest as it is involved in gibberellin biosynthesis; its structure serves as a test of the hypothesis that the αβγ-domain in plant αβγ diterpene synthases might have arisen from a bacterial diterpene synthase. Their work used **BL13B1**, **BL13C1** and **BL15A1** at the TLS.

Rv3378c catalyzed the condensation of adenosine and TPP to generate 1-TbAd (Fig. 1(a)).[5] The crystal structures of Rv3378c in apo-form and in a complex with its substrate TPP were solved here (Figs. 1(b) and 1(c)). These workers obtained also Rv3378c in a complex with a bisphosphonate inhibitor (BPH-629), in which one molecule occupied the TPP substrate-binding site and a second is located at the dimer interface (Fig. 2). These structures will help guide further antibiotic design against *M. tuberculosis*.

Fig. 1: Structures of Rv3378c. (a) Catalysis of Rv3378c. (b) Rv3378c ligand binding site. (c) Rv3378c/TPP (yellow, electron density contoured at 1.5σ) complex structure.

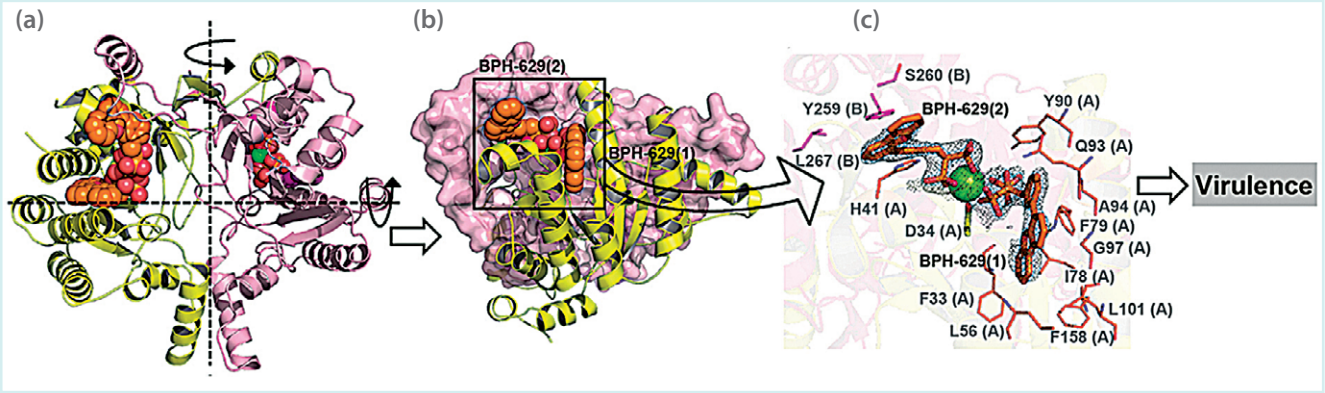

Fig. 2: Inhibitor-bound structures of Rv3378c. (a) Dimeric Rv3378c structure with four bound BPH-629 molecules. (b) Front view of Rv3378c dimer. (c) Close-up view of the structure of Rv3378c bound to bisphosphonate inhibitor BPH-629.

The structure of BjKS is similar to that found in the α domain in plant diterpene cyclases, indicating that modern plant terpene cyclases might have arisen from a fusion of the genes of ancestral (bacterial) α and βγ domain proteins. In addition, the structure of a diterpene diphosphate (*ent*-copalyl diphosphate) bound to a diterpene cyclase helps define the diterpene cyclase substrate-binding site (Fig. 3(a)). Three residues D75, D79 and R204 are confirmed to be essential for catalysis on using site-directed mutagenesis (Fig. 3(b) and 3(c)). The same aromatic bisphosphonate inhibitor used for the study of Rv3378c (BPH-629) was found to bind in the *ent*-CPP diphosphate-binding site and thus might be used as a potential plant-growth regulator (Fig. 3(d)).

References

1. M. Koksal, H. Hu, R. M. Coates, R. J. Peters, and D. W. Christianson, Nat. Chem. Biol. **7**, 431 (2011).
2. M. Koksal, Y. Jin, R. M. Coates, R. Croteau, and D. W. Christianson, Nature **469**, 116 (2011).
3. H. C. Chan, X. Feng, T. P. Ko, C. H. Huang, Y. Hu, Y. Zheng, S. Bogue, C. Nakano, T. Hoshino, L. Zhang, P. Lv, W. Liu, D. C. Crick, P. H. Liang, A. H. Wang, E. Oldfield, and R. T. Guo, J. Am. Chem. Soc. **136**, 2892 (2014).
4. W. Liu, X. Feng, Y. Zheng, C. H. Huang, C. Nakano, T. Hoshino, S. Bogue, T. P. Ko, C. C. Chen, Y. Cui, J. Li, I. Wang, S. T. Hsu, E. Oldfield, and R. T. Guo, Sci. Rep. **4**, 6214 (2014).
5. E. Layre, H. J. Lee, D. C. Young, A. J. Martinot, J. Buter, A. J. Minnaard, J. W. Annand, S. M. Fortune, B. B. Snider, I. Matsunaga, E. J. Rubin, T. Alber, and D. B. Moody, Proc. Natl. Acad. Sci. USA **111**, 2978 (2014).

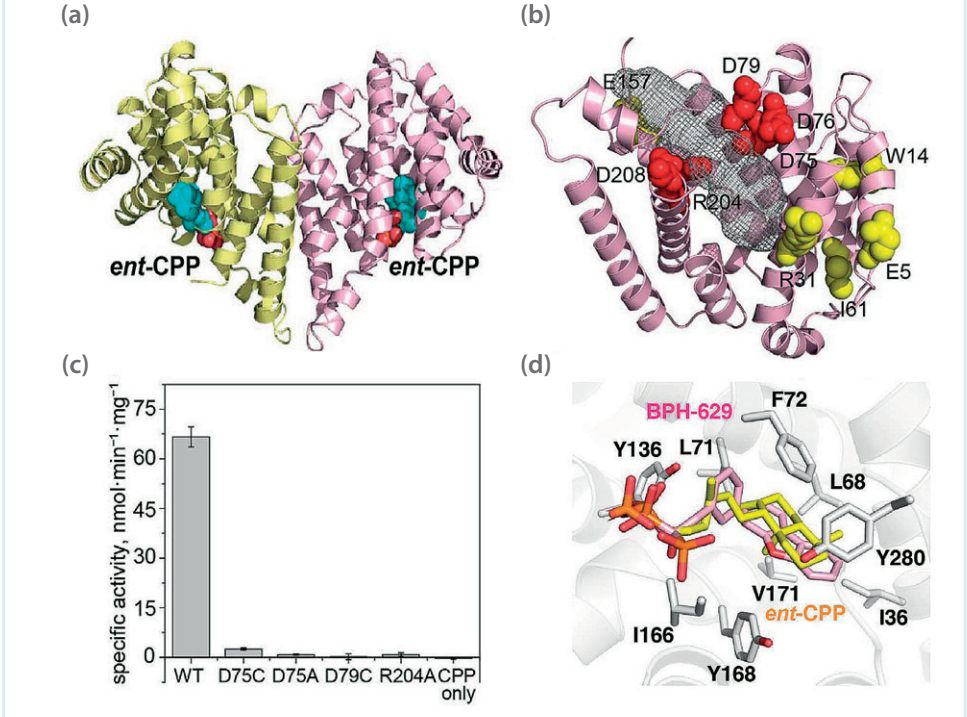

Fig. 3: Binding site, essential residues, and inhibition. (a) Stereo-view of *ent*-CPP bound structure (PDB ID 3WBV). (b) Highly conserved residues; residues in red mutated to A or C. (c) Activity of wild-type and mutant proteins. (d) Stereo-view of *ent*-CPP and BPH-629 in the BjKS active site.